Non-senescent keratinocytes organize in plasma membrane submicrometric lipid domains enriched in sphingomyelin and involved in re-epithelialization

Mound, Abdallah; Lozanova, Vesela; Warnon, Céline; Hermant, Maryse; Robic, Julie; Guere, Christelle; Vie, Katell; Lambert de Rouvroit, Catherine; Tyteca, Donatienne; Debacq-Chainiaux, Florence; Poumay, Yves

Published in:
Biochimica et Biophysica Acta - Molecular and Cell Biology of Lipids

DOI:
10.1016/j.bbalip.2017.06.001

Publication date:
2017

Document Version
Publisher's PDF, also known as Version of record

BBA - Molecular and Cell Biology of Lipids 1862 (2017) 958–971

Contents lists available at ScienceDirect

BBA - Molecular and Cell Biology of Lipids

journal homepage: www.elsevier.com/locate/bbalip

Non-senescent keratinocytes organize in plasma membrane submicrometric lipid domains enriched in sphingomyelin and involved in re-epithelialization

Abdallah Mound[a], Vesela Lozanova[a], Céline Warnon[b], Maryse Hermant[a], Julie Robic[c], Christelle Guere[c], Katell Vie[c], Catherine Lambert de Rouvroit[a], Donatienne Tyteca[d], Florence Debacq-Chainiaux[b,1], Yves Poumay[a,*,1]

[a] URPHYM, Namur Research Institute for Life Sciences (NARILIS), University of Namur, Namur, Belgium
[b] URBC, Namur Research Institute for Life Sciences (NARILIS), University of Namur, Namur, Belgium
[c] Laboratoires Clarins, Pontoise, France
[d] CELL Unit, de Duve Institute and Université Catholique de Louvain, Brussels, Belgium

ARTICLE INFO

Keywords:
Lipid submicrometric domains
Keratinocytes
Senescence
Sphingomyelin
Cholesterol
Keratinocyte migration

ABSTRACT

Membrane lipid raft model has long been debated, but recently the concept of lipid submicrometric domains has emerged to characterize larger (micrometric) and more stable lipid membrane domains. Such domains organize signaling platforms involved in normal or pathological conditions. In this study, adhering human keratinocytes were investigated for their ability to organize such specialized lipid domains. Successful fluorescent probing of lipid domains, by either inserting exogenous sphingomyelin (BODIPY-SM) or using detoxified fragments of lysenin and theta toxins fused to mCherry, allowed specific, sensitive and quantitative detection of sphingomyelin and cholesterol and demonstrated for the first time submicrometric organization of lipid domains in living keratinocytes. Potential functionality of such domains was additionally assessed during replicative senescence, notably through gradual disappearance of SM-rich domains in senescent keratinocytes. Indeed, SM-rich domains were found critical to preserve keratinocyte migration before senescence, because sphingomyelin or cholesterol depletion in keratinocytes significantly alters lipid domains and reduce migration ability.

1. Introduction

The heterogeneity of plasma membrane and organization, as well as their local specializations into signaling platforms have been proposed, based on various analytical techniques and observations, intending to attribute specific functions to specialized membrane areas [1]. Among lipid membrane components, cholesterol and sphingolipids are concentrated in special lipid domains characterized for instance by local reduced fluidity of the membrane [2], or by association with specialized proteins like caveolins [3], and possibly involved in highly specific functions like those of striated muscle T-tubules [4]. Often named 'lipid rafts', and defined as "small, heterogeneous, highly dynamic, sterol- and sphingolipid-enriched domains that compartmentalize cellular processes" [5], lipid-rich domains can either be evidenced in cellular membranes by their particular resistance to detergents [6], by their association with caveolins and flotillin, or by their low density when analyzed through isopycnic separation of membrane fragments [7]. Microscopic demonstrations of such specialized domains have for long required rather sophisticated techniques and have been often performed by analysis of artificial membranes [8]. Recently developed fluorescent probes however have nowadays proven that specialized submicrometric lipid membrane domains, enriched in sphingomyelin and/or cholesterol, can be visualized using confocal microscopy at the membrane of erythrocytes [9–13].

Trying to understand whether these cholesterol- and sphingomyelin-enriched plasma membrane domains can influence human keratinocytes in perception of their environment, we used the fluorescent probes to analyze for the first time adherent epidermal cells. The

Abbreviations: SM, sphingomyelin; SMase, sphingomyelinase; BODIPY-SM, *N*-(4,4-difluoro-5,7-dimethyl-4-bora-3a,4a-diaza-*s*-indacene-3-pentanoyl) sphingosyl phosphocholine; NBD-SM, *N*-[6-[(7-nitro-2-1,3-benzoxadiazol-4-yl)amino]hexanoyl]-sphingosine-1-phosphocholine; SA-βgal, senescence-associated β-galactosidase; CPD, cumulative population doublings; aSMase, acid sphingomyelinase; nSMase1, neutral sphingomyelinase 1; SMS2, sphingomyelin synthase 2; EGFR, epidermal growth factor receptor; MβCD, methyl-β-cyclodextrin

* Corresponding author at: University of Namur, Research Unit for Molecular Physiology (URPHYM)-NARILIS, 61 Rue de Bruxelles, B-5000 Namur, Belgium.
E-mail address: yves.poumay@unamur.be (Y. Poumay).
[1] Co-senior author.

http://dx.doi.org/10.1016/j.bbalip.2017.06.001
Received 27 January 2017; Received in revised form 26 April 2017; Accepted 3 June 2017
Available online 06 June 2017

first step was to detect whether lipids like cholesterol or sphingomyelin (SM) do cluster or not into lipid microdomains in keratinocyte membranes. Thus, procedures initially developed for erythrocytes were adapted for studies of adherent keratinocytes. To avoid potential mistakes due to eventual curvatures of the plasma membrane (e.g. in microvilli), observations were exclusively performed while focusing on the membrane anchored to the perfectly flat culture substratum. The basal membrane in cultured keratinocytes is indeed likely the only one being planar enough for trustable identification of submicrometric lipid domains using the above-mentioned approach in a confocal microscope.

In human skin, the barrier requires epidermal homeostasis involving keratinocytes proliferation, migration, and differentiation. The epidermal cell turnover becomes affected by aging as it slows down for instance in the elderly [14,15]. Perception of environmental information and consecutive adaptive cell responses happen through the keratinocyte plasma membrane, for instance by means of activation of signaling receptors or by engagement of adhesive transmembrane proteins. Interestingly, receptors and adhesive proteins are believed to localize in specialized membrane areas, where several actors gather in platforms devoted to control proliferation, differentiation, but also migration, potentially creating abnormal phenotypes in human keratinocytes and altering thereby the epidermal barrier [16,17]. Thus, the second step in this study was to investigate whether lipid domains are involved during senescence of epidermal keratinocytes, in correlation with eventual altered functioning.

Data hereby illustrate that cholesterol- and sphingomyelin-enriched submicrometric lipid domains can actually be visualized in keratinocytes, at least in basal membranes. They further indicate that lipid domains are perturbed during cell senescence and conversely preserved as long as keratinocyte senescence is prevented. Data also suggest that the functionality of lipid domains in keratinocytes depends not only on cholesterol, but also on SM.

2. Materials and methods

2.1. Cell culture and induction of replicative senescence

Human primary keratinocytes were isolated by the trypsin float technique from adult abdominal (NAK) and young foreskin (NFK) skin samples as previously described [18]. Samples were obtained after plastic surgery (donors over 52 years old, Dr. B. Bienfait, Clinique St. Luc, Namur-Bouge, Belgium) or circumcision (donors under 7 years old, Dr. L. de Visscher, Clinique St. Luc, Namur-Bouge, Belgium) following approval by the ethics committee of the Clinique St-Luc (Namur-Bouge) and informed consent of donors or representatives. Epidermal keratinocytes were isolated and cultured at 37 °C under a 5% CO_2 atmosphere in Epilife medium, containing human keratinocyte growth supplement (HKGs, Cascade Biologics, Mansfield, UK). Immortalized hTERT-keratinocytes were a kind gift from Pr. J. Rheinwald (Boston, USA) [19]. Senescence was induced in keratinocytes by keeping proliferative cells in culture for multiple passages, as previously described [20]. Subconfluent proliferative cells at 80% of cell density were trypsinized as described [18] and the cumulative cell population doublings calculated for each passage by determination of the number of divisions. The cultures were considered senescent when cells exhibit slower proliferation for two weeks and express senescence-associated β-galactosidase (> 80% of SA-βgal positive cells).

2.2. Cell treatments

For cholesterol depletion, confluent keratinocyte cultures were washed with PBS and then treated for 1 h at 37 °C with 7.5 mM methyl-β-cyclodextrin (MβCD) (Sigma-Aldrich, Diegem, Belgium) in culture medium, followed by incubation in basic culture medium for different periods (recovery times), as previously described [21]. For SM depletion, keratinocytes were treated at 20 °C with 5 mU/ml of *Bacillus cereus* sphingomyelinase (SMase; Sigma-Aldrich, Diegem, Belgium) for 10 min. For observation of lipid submicrometric domains, MβCD- and SMase-treated keratinocytes were labelled while keeping MβCD or SMase (as appropriate) in their medium. For treatment with Rho kinase inhibitor, keratinocytes were continuously maintained in normal medium supplemented with 10 μM of Y27632 compound.

2.3. Keratinocyte labelling with fluorescent probes

Human keratinocytes were seeded at 20,000 cells/cm^2 in Lab-Tek chambers (Thermo Fisher Scientific, NY, USA) and cultured in Epilife medium for 48 h. Before each experiment, BODIPY-SM (0.5 μM (*N*-(4,4-difluoro-5,7-dimethyl-4-bora-3a,4a-diaza-*s*-indacene-3-pentanoyl) sphingosyl phosphocholine); Thermo Fisher Scientific, NY, USA), NBD-SM (5 μM (C6-NBD sphingomyelin: *N*-[6-[(7-nitro-2-1,3-benzoxadiazol-4-yl)amino]hexanoyl]-sphingosine-1-phosphocholine); Biotium, CA, USA), lysenin* (1.25 μM), theta* (1.25 μM) or Vybrant DiIC18 (5 μM; Thermo Fisher Scientific, NY, USA) probes were mixed with medium supplemented with equimolar defatted bovine serum albumin (DF-BSA; Sigma-Aldrich, Diegem, Belgium) and then cleared from aggregates by centrifugation at 14,000 × *g* for 5 min. For surface labelling, cells were washed twice with medium at 4 °C, then incubated for 15 min with the probe solution at 4 °C, except otherwise stated. Following cell surface labelling, keratinocytes were washed 4 times with medium at 4 °C, then placed in medium at 20 °C and analyzed under confocal microscopy (Leica) at the level of planar basal membranes. For surface back-exchange procedure, keratinocytes were treated with 5% bovine serum albumin (BSA) at 4 °C prior to analysis. For each probe, images were recorded using 16% laser power in a Leica confocal microscope and 100 × magnification. For double labelling, data were sequentially acquired in green (488 nm), then red (568 nm) channels. To quantify the probe's co-localization, Pearson's coefficients between different labellings were calculated by Leica LAS-AF-Lite software over a minimum of 10 images from three independent experiments.

2.4. Image analysis

Lipid submicrometric domains were quantified using Visilog software (Thermo Fisher Scientific, Waltham, MA, USA). A special program has been created with an algorithm following three steps: i) denoising, ii) segmentation and iii) measurements. The process can be seen in Supp. Fig. 3. To remove the noise, a bilateral filter was applied to smooth the image while preserving the edges. Cell membranes were removed using morphological openings by linear structural elements oriented with several orientations. Then, a toggle filter enabled removal of the remaining impulsive noise and enhancement of the contrast. Images were finally binarized using a global threshold and the small components are removed. Three measures were computed:

1) The average number of lipid submicrometric domains per cell was computed by dividing the number of objects in the image by the number of cells. The number of cells was counted manually by an expert.
2) The average area of lipid submicrometric domains was calculated by dividing the total areas of lipid submicrometric domains in the image by the number of objects in the image.
3) The average intensity of lipid submicrometric domains was computed by dividing the intensity of the image by the area of the image.

2.5. Lipid extraction and quantification

Confluent cells in 60 mm standard cell culture dishes were scraped into 1 ml of demineralized water before being sonicated for 1 min. Lipids were then separated from proteins by extraction in chloroform/

methanol (2:1), followed by centrifugation for 15 min at 3000 rpm at room temperature (RT). NaCl (0.05 M) was added to the collected organic phase, which was then washed twice with 0.36 M $CaCl_2$/methanol (1:1). After stirring and centrifugation (15 min, 3000 rpm, RT) Triton X-100 (1% in acetone) was added to the organic phase and then evaporated under air flow using SpeedVac SC100 (Thermo Electron Corporation, Zellik, Belgium). The extracts were then resuspended in water. Cholesterol was quantified using the Amplex Red Cholesterol Assay Kit (Invitrogen, Merelbeke, Belgium) and SM by the Fluorometric Sphingomyelin Assay Kit (Abcam, Cambridge, UK) in accordance with instructions from manufacturers. Results were normalized to protein concentration measured in each sample.

2.6. Immunofluorescence

Keratinocytes were cultured in Lab-Tek chambers, labelled by lysenin*, examined under confocal microscopy as described above, then immediately fixed and immune-labelled using $p16^{INK-4A}$-(1:100) or EGFR-(1:100) specific antibodies. Briefly, after three washes in PBS, cells were fixed in 4% formaldehyde for 10 min at RT. Cells were then washed twice in PBS, permeabilized with PBS-Triton X-100 (1%, 5 min), saturated in PBS containing 1% BSA for 60 min and incubated with primary antibody for 2 h at RT, then rinsed before incubation with an Alexa Fluor secondary antibody for 1 h in the dark at RT before washes and observation under confocal microscopy.

2.7. Cell migration in scratch wound assays

Keratinocytes were cultured until confluent, then the monolayer was scraped with a p200 micropipette tip in a straight line to create a cell-free “scratch”. Cultures were then washed twice with PBS to remove cell debris, then cultured for recovery in fresh medium. The migration path of cells at the leading edge of the scratch was tracked using time-lapse imaging with Iprasense Cytonote device (Iprasense, Montpellier, France). Images from time-lapse sequences were analyzed with Horus software. Keratinocytes in the scratch assay were first treated with mitomycin C (10 μg/ml) to inhibit cell proliferation.

2.8. RNA extraction and RT-qPCR

Total RNA was extracted using a High Pure RNA isolation kit (Roche, Basel, Switzerland) following the manufacturer's instructions. SuperScript II kit (Life Technologies, California, USA) was used to reverse-transcribe 1 μg of total RNA. Complementary DNA was diluted 25-fold and amplification reaction was performed using SYBR Green Mastermix (Roche Diagnosis, Mannheim, Germany). Relative abundance of mRNA was quantified based on Ct difference [22] on a 7300 real-time PCR machine (Life Technologies) and normalized using RPLP0 gene. Sequences of primers used are (For. 5′-GCC CAA CGC GAA TAG T-3′ and Rev. 5′-CGC TGC CCA TCA TCA TGAC-3′) for $p16^{INK4a}$, (For. 5′-GCC CAA TCT GCA AAG GTC TATT-3′ and Rev. 5′-CCC ACG CGA GCC ACA T-3′) for acid sphingomyelinase (aSMase), (For. 5′-CAG GAC TTC CAG TAC CTG AGA CAG A-3′ and Rev. 5′-GGC CAC TGC CAA TGA TTC C-3′) for neutral sphingomyelinase 1 (nSMase1), (For. 5′-CCT GTG CCT GGA ATG CAT TT-3′ and Rev. 5′-ATC AAT CGT AGA ATC CGT TGA ACT T-3′) for sphingomyelin synthase 2 (SMS2) and (For. 5′-ATC AAC GGG TAC AAA CGA GTC-3′ and Rev. 5′-CAG ATG GAT CAG CCA AGA AGG-3′) for RPLP0.

2.9. Statistical analyses

Results were expressed as mean ± SD. Experiments were repeated at least 3 times. The one way analysis of variance (ANOVA) with Bonferroni post-hoc analysis were used to group comparison. Statistical significance is indicated in the figures as follows: NS, not significant; * = $P < 0.05$; ** = $P < 0.01$; *** = $P < 0.001$.

2.10. Reagents

Rabbit monoclonal antibody against EGF receptor was purchased from Cell Signaling (Leiden, The Netherlands; Cat#: 4267), rabbit polyclonal antibody against ribosomal protein L13a (RPL13a) was purchased from Cell Signaling (Leiden, The Netherlands; Cat#: 2765), and rabbit monoclonal antibody against $p16^{INK4a}$ (RPL13a) was purchased from LifeSpan BioScience (Seattle, WA, USA; Cat#: LS-B8693). All other reagents were from Sigma unless otherwise stated. Final concentrations were obtained by appropriate dilution of stock solutions so that the solvent never exceeded 0.1%.

3. Results

3.1. Keratinocytes organize SM- and cholesterol-rich submicrometric domains in their basal membrane

In recent studies, approaches using fluorescent probes were successfully used to visualize lipid submicrometric domains in red blood cell membranes (RBC). Experimental procedures were based either on plasma membrane insertion of an exogenous BODIPY-Sphingomyelin analog (BODIPY-SM) [11,23], or conversely on probing respectively endogenous SM or endogenous cholesterol by means of non-toxic fragments of lysenin [10] or theta toxin [9] which were rendered fluorescent by fusions with mCherry and hereafter named lysenin* and theta*. Visualization of lipid submicrometric domains in RBC plasma membrane took benefit of featureless smooth cell surfaces in this cell type, i.e. surfaces free of membrane protrusions like microvilli, thereby avoiding signal-enriched local areas which would have been impossibly distinguished from lipid-enriched domains in plasma membranes [12]. In the present work, those fluorescent probes were utilized in adapted protocols for the visualization of lipid submicrometric domains in plasma membranes of living human keratinocytes, focusing on their basal surface in order to avoid any membrane protrusions [1]. Thus, using low concentration of BODIPY-SM (0.5 μM) or non-saturating concentration of lysenin* (1.25 μM), SM-rich submicrometric domains were first identified at the basal surface of living keratinocytes. A similar approach using theta* was used to probe endogenous cholesterol and also reveal domains enriched in this molecule. Insertion of BODIPY-SM in the plasma membrane of living keratinocytes reveals SM-attractive domains observed by confocal microscopy in their basal membrane (Fig. 1A–C; Video 1). The presence of domains able to incorporate BODIPY-SM in plasma membrane was first confirmed by the disappearance of labelling in such domains upon surface back-exchange using 5% BSA (Fig. 1D). This procedure removes BODIPY-SM from the surface membrane only, while preserving probes internalized in endosomes when carried out at 20 °C (Fig. 1E). In addition, domains able to attract BODIPY-SM in plasma membrane were found to be sensitive to cholesterol depletion by methyl-beta-cyclodextrin (MβCD; resulting in ~ 50% of total cholesterol depletion), indicating that cholesterol is essential for the organization of SM-rich submicrometric domains (Fig. 1F). In the view to demonstrate that BODIPY-SM submicrometric domains do not reflect some surface structures in the basal membrane of keratinocytes we also analyzed the organization of DiIC18, a non-specific membrane marker (Fig. 2). Our results show that the distribution of this probe in the basal membrane of keratinocytes does not correspond to the patches labelled by insertion of BODIPY-SM into submicrometric domains.

Endogenous SM was then labelled by lysenin* and produced a pattern similar to the one observed after BODIPY-SM insertion, further suggesting elevated concentration of SM inside particular lipid submicrometric domains in keratinocyte basal membrane (Fig. 3A, C; Video 2). Interestingly lysenin* labelling is heterogeneous between different cells, suggesting some variation in SM concentration in plasma membrane between keratinocytes, revealing heterogeneity in the cell population. Lysenin*-labelling was abrogated by incubation of

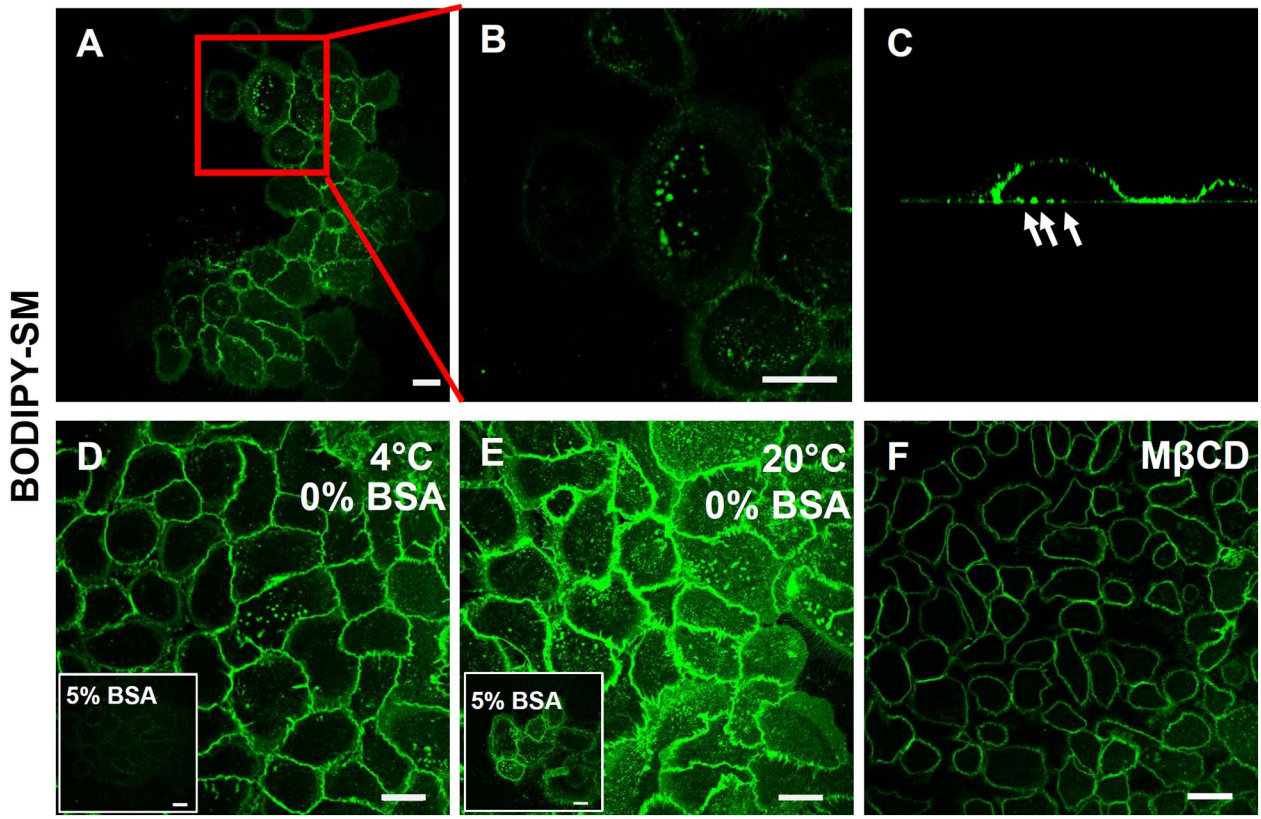

Fig. 1. BODIPY-SM concentrates into lipid submicrometric domains in keratinocytes: A. Living keratinocytes were cultured up to confluence in Lab-Tek chambers, then labelled by insertion of exogenous 0.5 μM BODIPY-SM at 4 °C (at 20 °C in panel E), and finally observed at 20 °C using confocal microscopy to focus on basal cell surface. B. Magnified microscopic area boxed in (A). C. Z-projection from 3D confocal image construction. The arrows indicate domains containing BODIPY-SM in basal keratinocyte membrane. D. BODIPY-SM labelled cells were submitted at 4 °C to a surface back-exchange procedure using 5% BSA (inset) and compared to results observed in control conditions (0% BSA). E. Same treatment and conditions as in (D) but at 20 °C. F. Methyl-β-cyclodextrin (MβCD; ~ 50% total cholesterol depletion) pretreated keratinocytes were surface-labelled with BODIPY-SM. Videos illustrating 3D structures of cells were constructed from Z-stack images of cells labelled by BODIPY-SM (see Video 1).

keratinocytes with SMase (Fig. 3A; insert), further demonstrating the specificity of the lysenin* probe. The fluorescent signal observed after incubation with lysenin* was also sensitive to cholesterol depletion (Fig. 3B), confirming the suggested role for cholesterol in organizing SM-rich domains in keratinocytes. Confocal imaging of keratinocytes treated by MβCD indicates that, as previously reported [24,25], cholesterol-depletion slightly alters the cell morphology and spreading (Figs. 1F and 3B).

Finally, keratinocytes probed by theta* reveal lipid submicrometric domains enriched in cholesterol. Confocal microscopy and an approach similar to the one used above to probe SM clearly indicated their localization also in the basal membrane of keratinocytes (Fig. 3D, F; Video 3). Cholesterol labelling disappears after cholesterol depletion by MβCD (Fig. 3D; inset), demonstrating specificity of the theta* probe used in this study. Interestingly, labelling by theta* was also slightly decreased as a result of SM depletion (Fig. 3E), suggesting that SM in turn can influence the organization of cholesterol in specialized domains of plasma membranes, in good accordance with recent data obtained while analyzing RBC [9].

3.2. Cholesterol partially co-localizes with SM in lipid submicrometric domains

A comparison of lipid submicrometric domains labelled by insertion of exogenous BODIPY-SM and by direct recognition using lysenin* or theta* was carried out in basal membrane of keratinocytes (Fig. 4). Because lysenin* can bind to both endogenous SM, as well as to exogenous BODIPY-SM [10], keratinocytes were initially labelled with lysenin*, then afterwards incubated with BODIPY-SM. SM-rich submicrometric domains labelled by lysenin* exhibit a partial co-localization with those gaining fluorescence by insertion of exogenous BODIPY-SM (Pearson's correlation coefficient $r = 0.8012 \pm 0.02$) (Fig. 4A), indicating propensity of keratinocytes to organize SM-rich submicrometric domains that can eventually be able to accumulate some more SM when available. Because SM-containing and cholesterol-containing domains seemed related to each other, as deduced from data described above, double labelling using theta* and BODIPY-SM was also performed. Such a procedure illustrates that part of the cholesterol-rich domains only can be labelled with BODIPY-SM (Fig. 4B, Pearson's correlation coefficient $r = 0.4597 \pm 0.04$), indicating that some heterogeneity, maybe in composition, does preclude lipid submicrometric domains from uniform behavior in keratinocytes.

Similar results were found using another exogenous NBD-Sphingomyelin (NBD-SM) fluorescent analog (Supp. Fig. 1). Indeed, as is observed when using BODIPY-SM, NBD-SM concentrates into submicrometric domains previously labelled by lysenin* (Supp. Fig. 1B) or by theta* (Supp. Fig. 1C). These NBD-SM attractive domains are again sensitive to cholesterol or SM depletion respectively by incubation with MβCD or with SMase (Supp. Fig. 1A).

Taken together, these data reveal lipid submicrometric domains with heterogeneous composition in living keratinocytes. In order to explore whether lipid domains identified by the above-mentioned labelling procedures can eventually be involved in some kind of cell signaling, immuno-localization of the epidermal growth factor receptor (EGFR) was performed in basal membrane of keratinocytes after previous SM-labelling with lysenin*. A proportion of EGFR was indeed found concentrated inside SM-rich domains (Supp. Fig. 2, Pearson's correlation coefficient $r = 0.3385 \pm 0.02$).

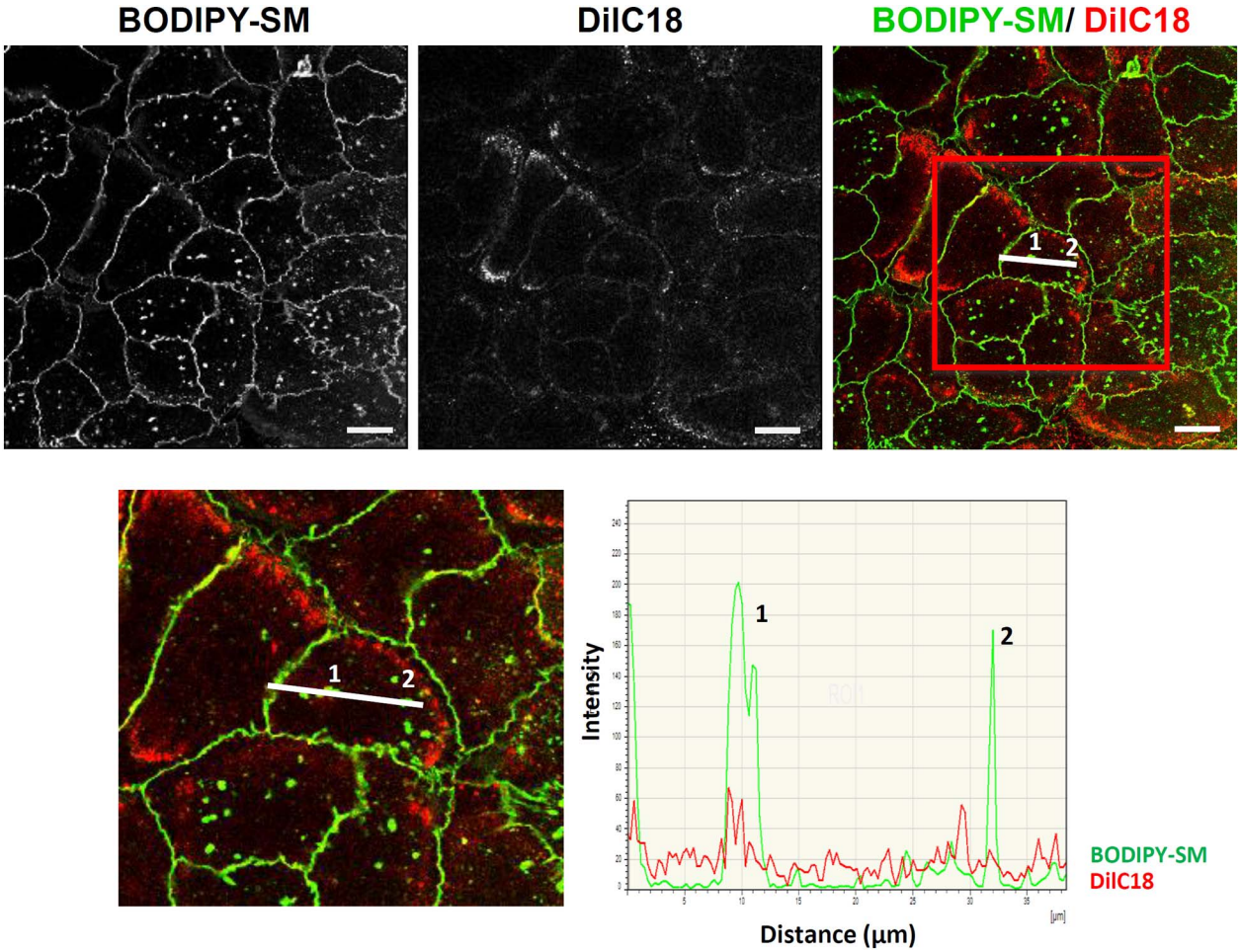

Fig. 2. Submicrometric BODIPY-SM domains do not reflect anatomical surface structures in living keratinocytes: living keratinocytes were examined after labelling with vibrant DiIC18 and BODIPY-SM for confocal imaging. Line intensity profiles of vibrant DiIC18 (red) and BODIPY-SM (green) signals were measured along the white traced line on the keratinocytes boxed at the bottom panel.

3.3. Replicative senescence in human keratinocytes suppresses the number of SM-rich submicrometric domains

In order to attribute some functionality to lipid domains, their presence during the proliferative lifespan of cultured keratinocytes and eventual defects in their maintenance during prolonged cell culture were analyzed over cumulative population doublings. Replicative senescence was induced in primary human keratinocytes using strains either isolated from adult abdominoplasties (NAK) or from infant foreskins (NFK). In both cases, keratinocytes were maintained as growing cultures, trypsinized while sub-confluent in order to prevent irreversible growth-arrest and differentiation that occur at keratinocyte culture confluence [18]. Proliferative lifespan was monitored by establishing cumulative population doublings (CPD) at each subdivision (Supp. Fig. 3A). Growth-arrest was observed in sub-confluent conditions after around 15 and 20 CPDs, respectively for NAK and NFK, corresponding to 12 passages, when the cell population reaches a senescence plateau [26]. Percentage of senescent cells was analyzed using an assay to detect senescence-associated beta-galactosidase (SA-βgal) activity during the lifespan of cultured keratinocytes [27,28]. When growth-arrested as a result of senescence, cell populations exhibit around 80% of SA-βgal-positive keratinocytes (Supp. Fig. 3B). Morphological analysis of SA-βgal-positive cells (stained blue) by phase-contrast microscopy (Supp. Fig. 3C) reveal increased numbers of enlarged keratinocytes among senescent cells [29,30]. Growth-arrest was further confirmed by elevated expression levels of $p16^{INK-4A}$-encoding mRNA with senescence (Supp. Fig. 3E) and the enhanced detection of $p16^{INK-4A}$ protein by Western blotting analysis (Supp. Fig. 3D). The $p16^{INK-4A}$ cyclin-dependent kinase inhibitor (CDKI) is responsible in keratinocytes for the major cell-cycle arrest that is concomitant with cell senescence in vitro [31], as well as in vivo [32].

Procedures described in this study for observation of lipid domains in cultured keratinocytes were then used to label SM- and cholesterol-rich membrane areas at early (P4) and late (P10) passages of NAKs. Both early passage (P4) and senescent (P10) NAKs display a certain number of submicrometric domains which are able to insert exogenous BODIPY-SM (Fig. 5A). However, lysenin*-labelling of identical cultures conversely exhibits less numerous domains that bind the fluorescent probe when the number of passages increases (i.e. labelling by lysenin* is observed in almost all P4 NAKs, but observed in a few cells only in P10 keratinocytes). Nevertheless, these SM-attractive submicrometric domains revealed by the insertion of BODIPY-SM in the senescent keratinocytes are sensitive to cholesterol depletion by MβCD (Supp. Fig. 4), suggesting that elevated cholesterol concentration is required to attract SM into keratinocyte plasma membranes.

These observations indicate that, despite the maintained potential for insertion of BODIPY-SM in plasma membrane, the number of keratinocytes labelled by lysenin* significantly decreases in late passages, particularly in characteristic enlarged senescent cells, suggesting suppressed synthesis of endogenous SM in such keratinocytes. Moreover, co-labelling of keratinocytes by lysenin* first in order to localize SM, then by immune detection of $p16^{INK-4a}$, reveals that their expression of this particular senescence marker is inversely related to the detection of endogenous SM. Enlarged senescent keratinocytes especially display

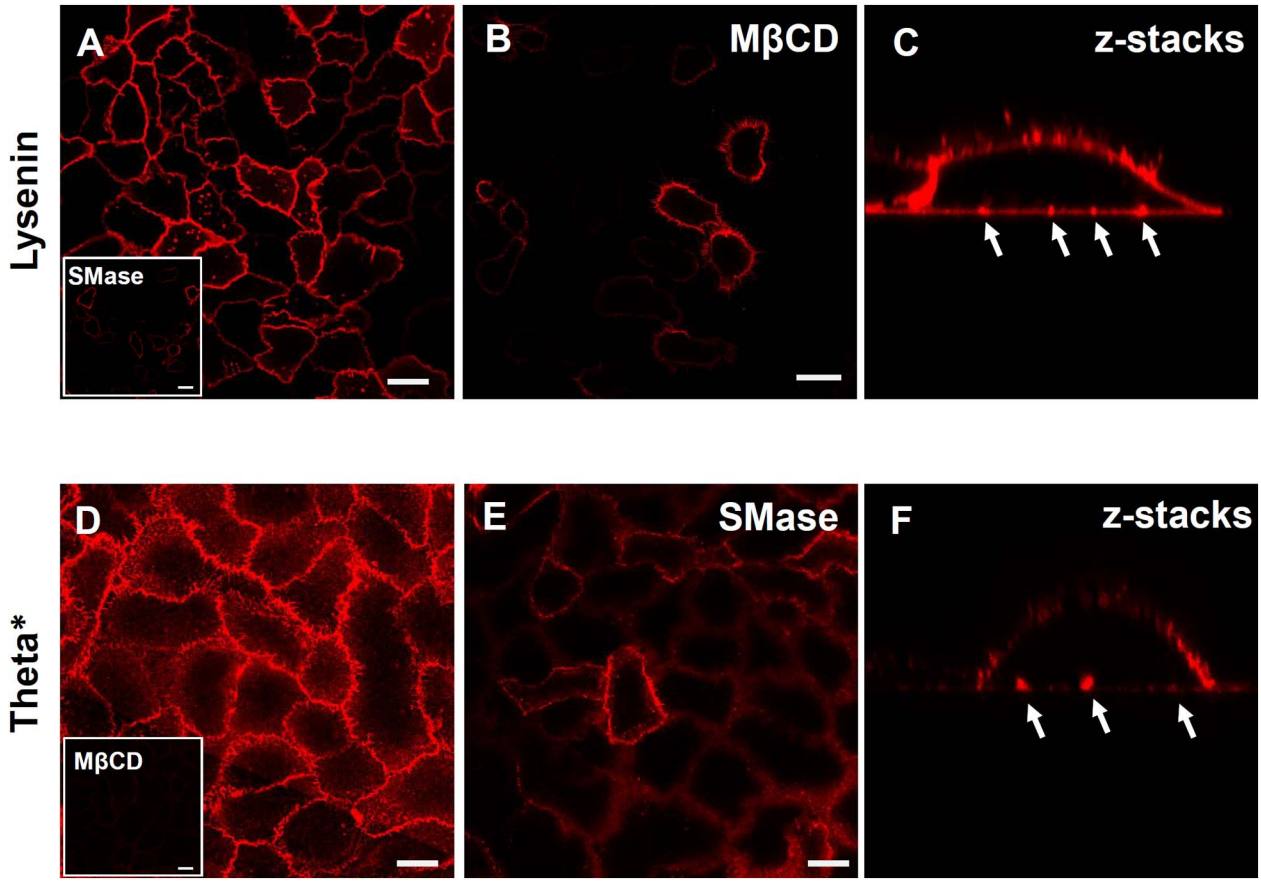

Fig. 3. Visualization of lipid submicrometric domains in keratinocytes: A. Living keratinocytes were cultured up to confluence in Lab-Tek chambers, then directly labelled at 4 °C for endogenous SM-rich micrometric domains with lysenin*, eventually after pretreatment with SMase (inset). B. Keratinocytes were identically labelled by lysenin* after incubation with MβCD. C. Z-projection from 3D confocal image construction produced after analysis of lysenin*-labelled keratinocyte. The arrows indicate SM-containing domains in basal membrane. D. Living keratinocytes were cultured up to confluence in Lab-Tek chambers, then directly labelled at 4 °C for endogenous cholesterol-rich micrometric domains with theta*, eventually after pretreatment with MβCD (inset). E. Identical labelling conditions as in J, but after SMase treatment. F. Z-projection from 3D confocal image construction produced after analysis of theta*-labelled keratinocyte. The arrows indicate cholesterol-containing domains in basal membrane. Videos illustrating 3D structures of cells were constructed from Z-stack images of cells labelled by lysenin* (see Video 2) or theta* (see Video 3). All scale bars, 20 μm.

lowered SM content while exhibiting elevated expression of $p16^{INK-4a}$ (Fig. 5B).

Because data suggest less numerous SM-rich submicrometric domains in senescent keratinocytes, their average number, labelling-intensity and surface area were quantitatively analyzed by computer-assisted morphometry. The results illustrate decreased number and less intense labelling of SM-rich submicrometric domains along the lifespan of NAKs (Fig. 6) and NFKs (Supp. Fig. 5). Conversely, the average surface area of domains remains unchanged. Simultaneously, the frequency of NAKs labelled by theta* is almost unchanged between early and late passages of cultured keratinocytes, indicating that cholesterol remains in rather stable amounts in keratinocyte membranes, along their entire lifespan (Fig. 7).

Finally, total lipid extraction was performed in order to measure SM and cholesterol keratinocyte content during senescence of this cell type. Data interestingly confirm lowered SM (Fig. 8A) and stable cholesterol (Fig. 8B) contents in keratinocytes when analyzed at elevated passages. Some decrease in SM content during keratinocyte senescence could either be explained by decreased synthesis, increased degradation, or both. To address this question, expression levels of mRNAs encoding acid sphingomyelinase (aSMase), neutral sphingomyelinase (nSMase1) or sphingomyelin synthase 2 (SMS2) were determined by RT-qPCR (Fig. 8C). Whereas the mRNA expression level for nSMase1 appears stable, the expression of aSMase is conversely enhanced in senescent keratinocytes. Simultaneously though, the expression level for SMS2 is reduced in senescent keratinocytes.

3.4. The number of SM-rich submicrometric domains is maintained in normal keratinocytes cultured in the presence of Y27632, as well as in immortalized NhTERT-keratinocytes

Potential inverse relationship between senescence and the presence of SM-rich domains in keratinocytes was further assessed in particular culture conditions which impede keratinocyte senescence.

Firstly, the Y27632 Rho kinase inhibitor was used for its reported potency to prevent loss of proliferation and senescence in keratinocytes [33]. NAKs were cultured for multiple passages in medium supplemented with 10 μM Y27632, then monitored for signs of senescence. Y27632 indeed extends the lifespan of normal keratinocytes in our hands too, as demonstrated by prolonged growth-phase (Supp. Fig. 6A) and reduced percentage of SA-βgal-positive cells (Supp. Fig. 6B, C).

Secondly, NhTERT-keratinocytes expressing telomerase and lacking functional $p16^{INK4a}$ [19] were identically analyzed. NhTERT-keratinocytes escape senescence, exhibiting constant proliferation, no appearance of SA-βgal activity, and unaltered morphology during cell culture for an elevated number of passages, either treated or not with Y27632 (Supp. Fig. 6D–F).

Thus, the organization of SM-rich lipid submicrometric domains were investigated in Y27632-treated NAKs and in NhTERT-keratinocytes, at increasing numbers of passages, using both insertion of BODIPY-SM and probing of endogenous SM using lysenin* (Fig. 9), as described above. Keratinocytes with extended lifespan due to Y27632 exhibit preserved SM-rich domains revealed by labelling with lysenin*,

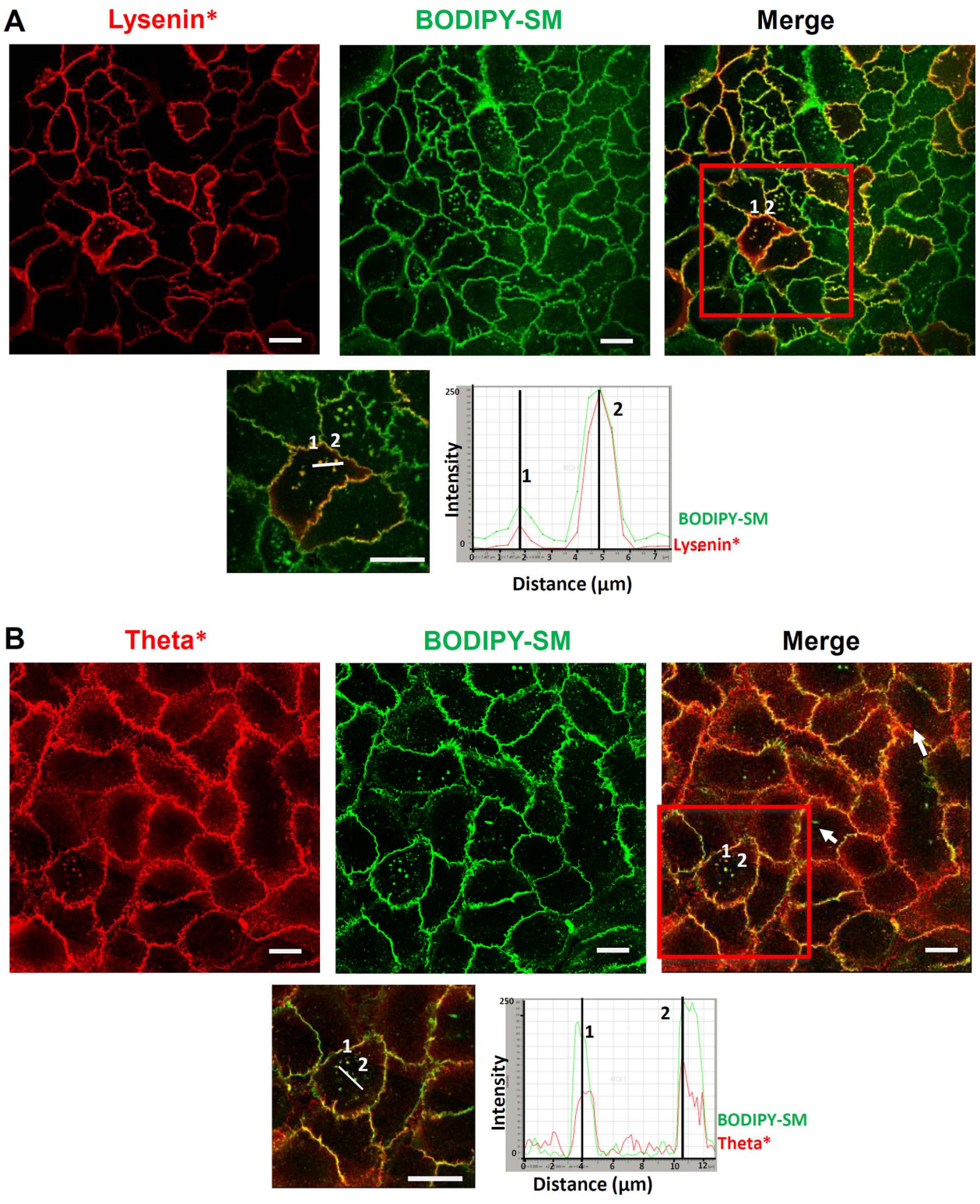

Fig. 4. SM-rich domains are associated with cholesterol: A. Living keratinocytes were labelled with lysenin*, then with BODIPY-SM. Line intensity profiles of lysenin* (red) and BODIPY-SM (green) signals were measured along the white traced line on the keratinocytes boxed at the bottom panel. Numbers indicate domains chosen to illustrate co-localization. B. Cells labelled by theta* exhibit partial co-localization between endogenous cholesterol-rich and submicrometric domains prone to incorporate BODIPY-SM. Line intensity profiles are shown in the bottom panel. Numbers indicate the chosen co-localized domains and arrows indicate domains labelled by BODIPY-SM or theta* only. All scale bars, 20 µm.

at least until P16 (Fig. 9A). Although several morphological changes appear after prolonged cultures of Y27632-treated keratinocytes, their labelling by lysenin* exhibits preserved numbers of SM-rich domains. Likewise, NhTERT keratinocytes exhibit constant SM-labelling and numbers of SM-rich submicrometric domains during long-term culture (Fig. 9B). Quantitation of total SM contents in both culture conditions further revealed unaltered levels for SM, even in cells analyzed in late passages (Fig. 9C). Simultaneously, cholesterol distribution and content were unaltered in Y27632-treated and hTERT-keratinocytes, but still depleted by MβCD (Supp. Fig. 7).

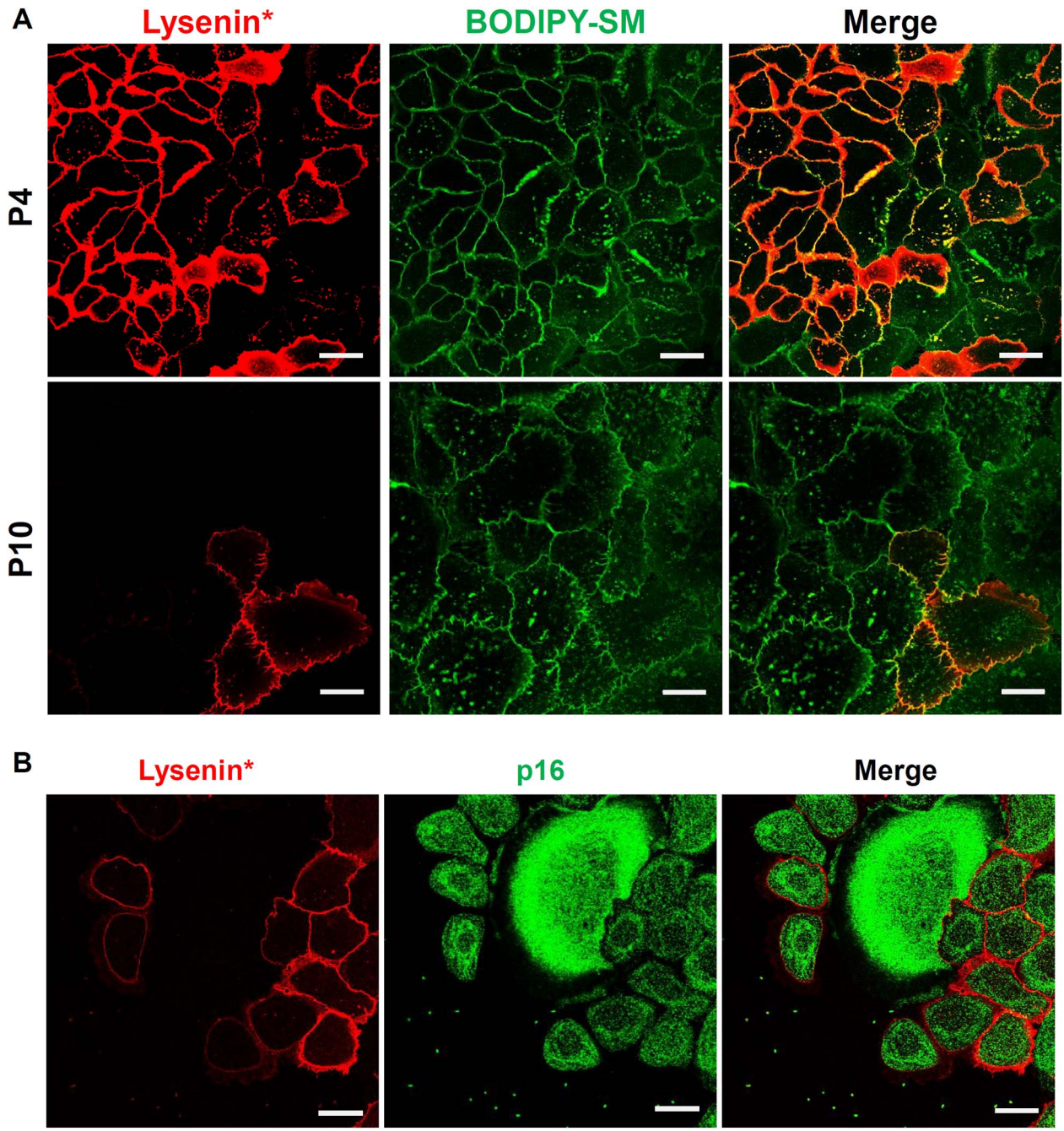

Fig. 5. SM-rich lipid domains become less frequent in keratinocyte membranes during replicative senescence: A. Normal human adult keratinocytes (NAK) were cultured for long-term in order to induce replicative senescence, than were double-labelled by lysenin* and BODIPY-SM at different passages. Passage 4 (P4) is illustrated as one example of pre-senescent keratinocytes and passage 10 (P10) was chosen to illustrate cells undergoing replicative senescence. B. NAK keratinocytes at passage 8 were labelled by lysenin* then immediately fixed and labelled by indirect immunofluorescence using an antibody against $p16^{INK-4A}$ and a secondary Alexa (green) antibody before observation under fluorescent microscopy.

3.5. Migration ability of keratinocytes relies on SM and cholesterol membrane contents and decreases during replicative senescence

Migration potential of untreated normal keratinocytes was monitored at different stages of replicative senescence using a wound healing scratch assay. Keratinocytes in a scratch assay were treated with mitomycin C (10 μg/ml) to inhibit cell proliferation, while preserving viability and ability to migrate. Data illustrate that senescent cells in passage 10 (P10) exhibit reduced migration ability when compared to cells of the same strain analyzed in passage 4 (P4) (Fig. 10A). Indeed, senescent keratinocytes slowly colonize the surface devoid of cells between the edges created by the scratch, in contrast with cells analyzed during early passages. Interestingly, trying to reproduce some alterations mentioned above in the lipid content and organization inside membranes of senescent keratinocytes, SM or cholesterol were depleted in early passage keratinocytes which were then analyzed for eventual consequences on their migration ability (Fig. 10B). While cholesterol depletion by MβCD (7.5 mM) evidently abolishes keratinocyte migration, degradation of SM in keratinocyte plasma membrane by incubation of cells with SMase (5 mU/ml) clearly slows down the process. Conversely, Y27632 which preserves the organization of SM-rich submicrometric domains during senescence is well known to simultaneously enhance cell migration, suggesting again possible links between SM organization in keratinocyte membranes and their propensity to migrate.

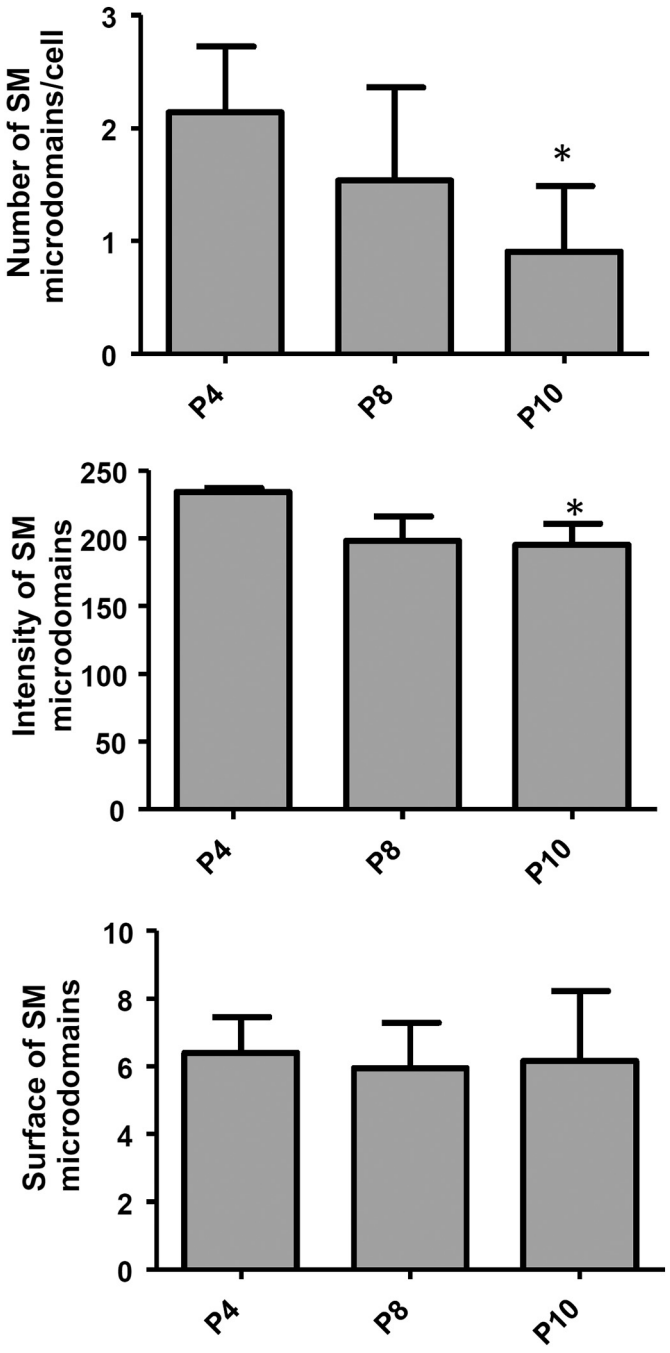

Fig. 6. Number and intensity of SM-rich submicrometric domains decrease during RS of human keratinocytes: NAKs keratinocytes cells were subcultured until reaching senescence, then images of cells labelled by lysenin* were analyzed (for further explanations, please see Materials and methods). The average number, the average intensity, and the average area of SM-rich submicrometric domains were measured at different passages.

4. Discussion

4.1. Overview

Cells interact with their environment through signals induced, for instance, by adhesion to the extracellular matrix, by growth factors or cytokines, thanks in both cases to integral receptor proteins inserted in plasma membrane, likely inside specialized domains. The classical membrane model has been constantly revised during the last two decades and has evolved into a model which definitely integrates heterogeneous domains enriched in special lipid and protein compositions dispersed in the more classical phospholipid bilayer, creating thereby signaling platforms on the cell surface [34]. Clear demonstration of such domains has been and is still a difficult technical matter, keeping their actual existence a sometimes controversial matter [35]. This study reports in a first part original visualization of lipid submicrometric domains in living cultured keratinocytes by mean of a procedure adapted from studies initially performed on RBC membranes [9–12]. In a second part, this study identifies functionality for such domains, but also their eventual disorganization and associated loss-of-function in senescent keratinocytes.

4.2. Lipid submicrometric domains can be visualized in basal membrane of living cultured keratinocytes

SM and/or cholesterol-rich lipid submicrometric domains in keratinocytes can be demonstrated by means of two approaches. The first one is based on insertion of a fluorescent BODIPY-coupled exogenous SM analog (BODIPY-SM) [12,23]. The second approach utilizes non-toxic fragments of lysenin and theta toxin, rendered fluorescent by protein fusion with mCherry, that specifically and respectively bind SM and cholesterol in plasma membranes of living cells [9,10]. Observations of lipids in adherent keratinocytes have been strictly limited to planar basal membranes in order to avoid potential bias eventually created by microvilli or other structural protrusions in plasma membranes and which could locally enhance fluorescence associated to membranes at the surface of cultured cells [1].

BODIPY-SM clusters into micrometric domains in living normal keratinocytes cultured under usual conditions [18]. Specificity of observations was assessed by several control experiments, confirming that SM-attractive domains depend on the presence of endogenous cholesterol and reside inside the plasma membrane of keratinocytes.

Affinity of specific submicrometric lipid domains for SM, as well as for cholesterol, was confirmed by specifically labelling endogenous SM [36] or cholesterol in membranes of living keratinocytes. In living keratinocytes, fluorescent lysenin* labels SM-rich submicrometric domains which are sensitive to SM depletion by sphingomyelinase activity, confirming the usefulness of lysenin* as a probe for SM in keratinocyte basal membrane. SM-rich domains were also found sensitive to cholesterol depletion by MβCD, indicating that cholesterol is essential to organize SM-rich lipid submicrometric domains in keratinocytes. Several studies previously demonstrated crucial involvement of cholesterol in other cell types to organize specialized membrane domains [10,23]. Interestingly, similar results were reported in a recent study which uses a totally different biophysical approach to identify lipids in plasma membranes [37]. However, those data rather suggest that cholesterol affects the organization of sphingolipids via an indirect mechanism which may involve the cytoskeleton [38].

Present data further reveal that SM-rich domains, identified by lysenin*-labelling, are able to host additional exogenous BODIPY-SM, showing that such domains do attract SM in membranes of anchored keratinocyte. These results were confirmed by using a different exogenous fluorescent SM analog (NBD-SM).

Conversely, because even a minor modification of cholesterol molecular structure appears sufficient to disturb distribution of this lipid in membranes [39], we discarded any utilization of the fluorescent cholesterol analog for this study, and rather preferred using fluorescent theta* toxin to probe endogenous cholesterol molecules accessible from the cellular environment. Using this approach, cholesterol is also found gathered into submicrometric domains inside membranes at the basal surface of living keratinocytes. As expected, cholesterol-rich domains are abrogated by incubation with MβCD, further proving specificity for theta* as a probe [9,40]. Cholesterol-rich domains are also sensitive to SM-depletion by SMase, suggesting that SM is somewhat required to stabilize cholesterol-rich submicrometric areas

In relation with potential functionality of lipid domains in keratinocyte signaling, EGF receptor is here reported as frequently localized inside SM-rich domains, in strong accordance with several reports that

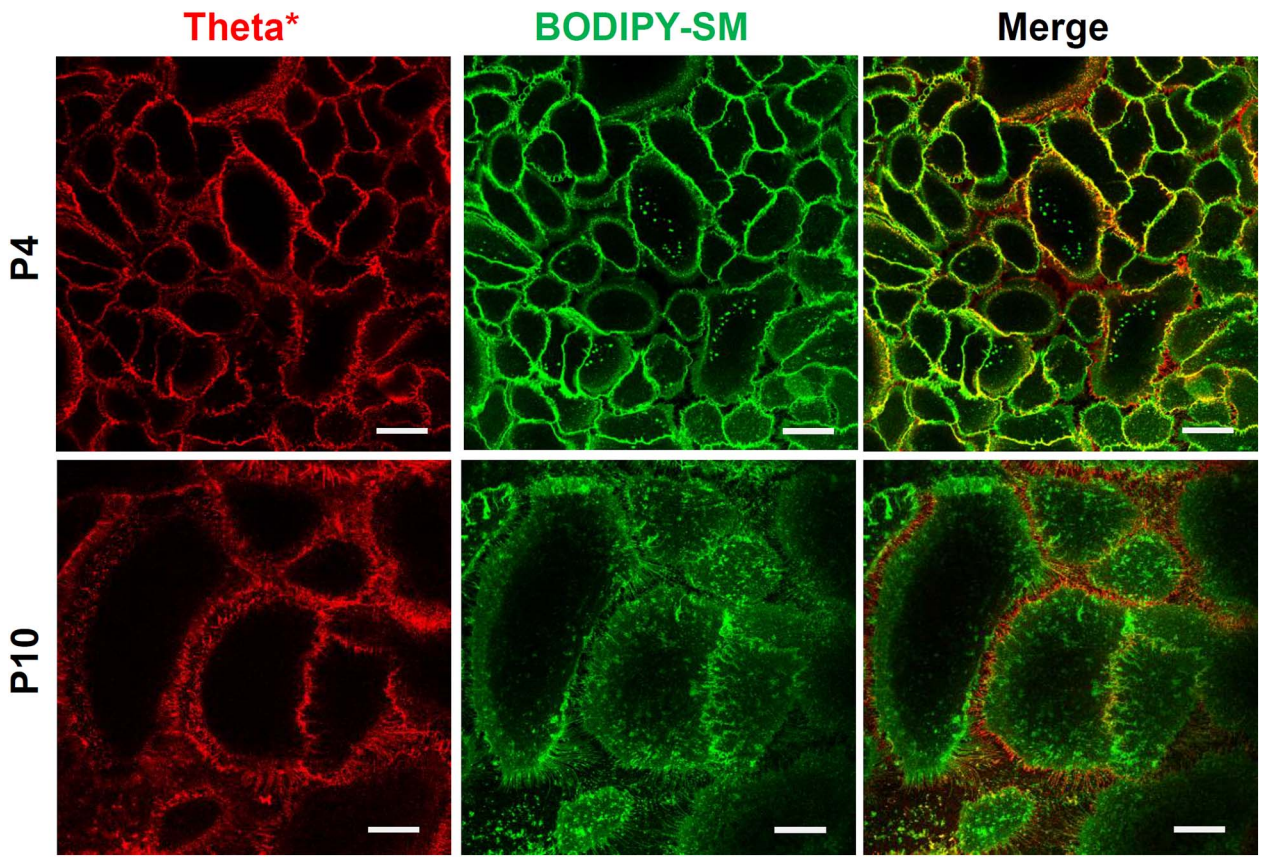

Fig. 7. Cholesterol-containing lipid domains seem unaltered in keratinocyte membranes during replicative senescence: normal human adult keratinocytes (NAK) were cultured for long-term in order to induce replicative senescence, than were double-labelled by theta* and BODIPY-SM at different passages. Passage 4 (P4) is illustrated as one example of pre-senescent keratinocytes and passage 10 (P10) was chosen to illustrate cells undergoing replicative senescence.

identified EGF receptor as part of specialized signaling platforms in plasma membrane [41,42]. This approach should now be extended to other receptors, as well as to specialized membrane areas, like apical structures or cell junctions.

Regarding intercellular junctions, it is interesting to note that pioneer research about desmosomal membrane components had already reported particularly elevated amounts of SM in purified desmosomes, in regard of other membrane areas [43]. Moreover, lipid microdomains were recently demonstrated being involved in dynamics of desmosomes [44], arguing to extend investigations into still unknown relationships between lipid domains and cell junctions.

4.3. SM is suppressed in membranes of senescent keratinocytes

The abundance of SM-rich domains decreases when replicative senescence occurs in keratinocytes, in concomitance with decreased SM detection, whereas cholesterol remains unaffected. However, our results demonstrate that exogenous BODIPY-SM is still able to concentrate into micrometric patches in senescent keratinocytes, suggesting preservation of SM-attractive submicrometric domains in these cells. Interestingly, the demonstration of SM-attractive submicrometric domains by the use of exogenous SM analogs requires cholesterol to organize such specialized lipid microdomains.

Involvement of lipids during aging, as well as in age-related diseases, has often been proposed. For instance, analyses of lipid concentrations (sphingomyelins, ceramides, and cholesterol) in brain tissues from mice reported increased content of free cholesterol and long-chain ceramides during aging [45,46]. In skin, while the lipid content could decrease with age [47], other studies conversely reported little or no relationship between aging and lipids [48,49]. Extending the lifespan of keratinocytes with Y27632 inhibitor was also found to preserve SM amounts and maintain SM-rich submicrometric domains. All these characteristics were also found in immortalized keratinocytes, suggesting potential roles for SM-rich domains in keratinocytes that escape senescence.

Although published data about senescent fibroblasts report that ceramide levels [50] and sphingomyelinase activity [51] might be involved in the aging process, available experimental data are not sufficient enough to provide a proper explanation for such SM alterations in keratinocytes.

Accumulation of senescent keratinocytes and fibroblasts with age [14,27] may explain altered responses to growth factors, hormones and cytokines [15,52–55] and decrease in both proliferation and differentiation potentials of keratinocytes, resulting into the well-known compromised healing processes in elderly people [54,56].

4.4. Keratinocyte abilities to migrate decrease during senescence, as well as after SM or cholesterol depletion

SM or cholesterol depletion from keratinocytes' plasma membrane reduces the ability of cells to migrate. This observation strongly suggests that lipid and lipid microdomains in cell membrane are playing crucial roles required for normal skin re-epithelialization and purposely regulated keratinocyte migration. Indeed, previous investigations demonstrated how physical membrane properties, which are highly influenced by lipid composition, can regulate cell migration [57,58]. Thereby, it has been shown for instance that angiogenic growth factors and some lipophilic molecules regulate cell motility through alterations in membrane properties and the redistribution of signaling molecules to membranes in endothelial cells [58]. Cholesterol depletion also revealed that this membrane component is crucial to the generation of some microviscosity gradient which increases in plasma membrane, at

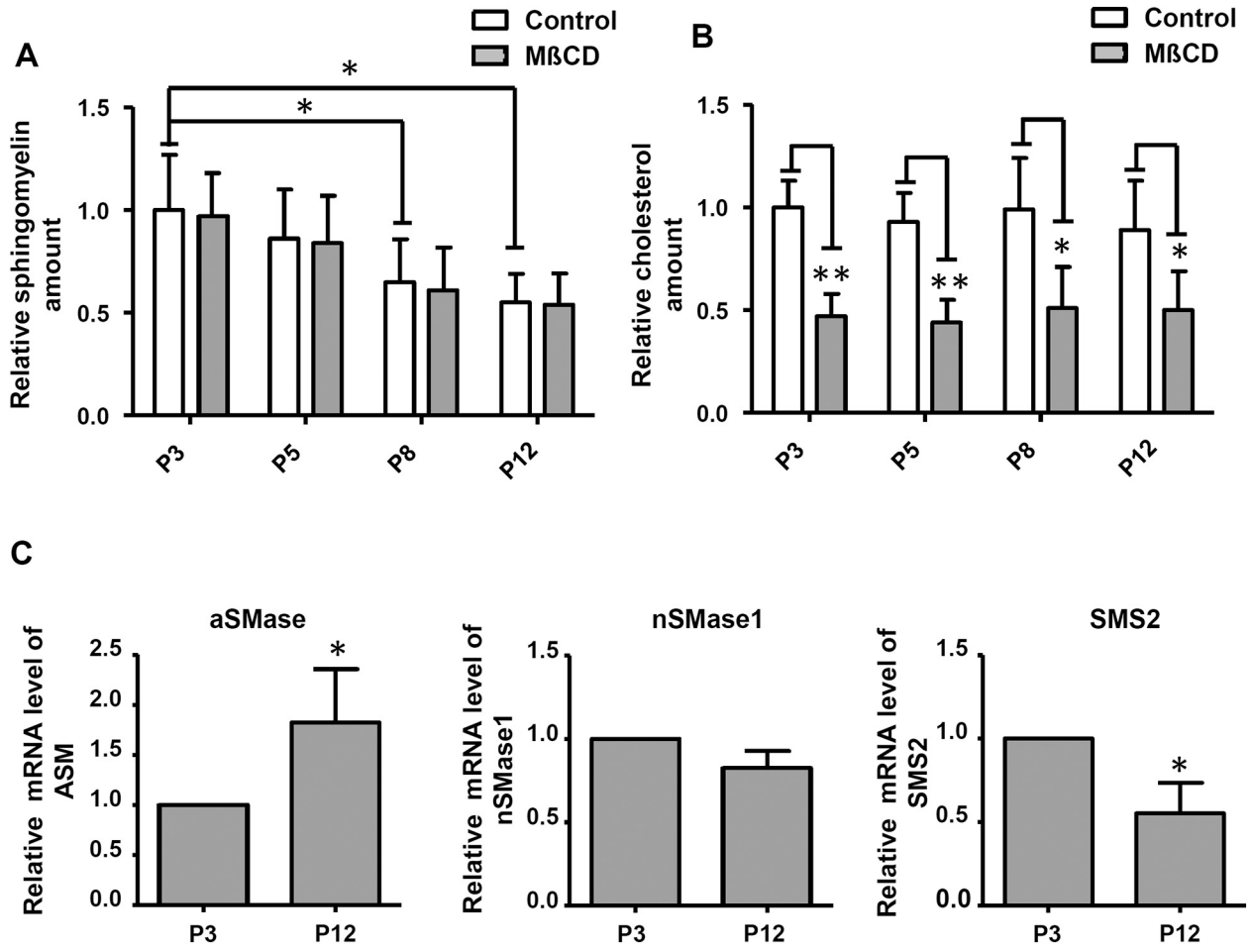

Fig. 8. Total amount of SM (but not of cholesterol) decreases during replicative senescence of human keratinocytes: total SM (A) and cholesterol (B) amounts were measured along passages of NAK, treated or not with 7.5 mM MβCD for 1 h. Measured values have been normalized to protein concentration in each sample and data are presented as means ± SD of three independent experiments. Their statistical significance is evaluated by ANOVA 1 after testing the homogeneity of variance (Bartlett) (*: $P < 0.05$, **: $P < 0.01$, ***: $P < 0.001$). Post-hoc comparisons were performed by pairwise Scheffe's test. C. Steady-state mRNA levels of acid sphingomyelinase (aSMase), neutral sphingomyelinase (nSMase1) and sphingomyelin synthase 2 (SMS2) were determined by RT-PCR. The RPLP0 stably expressed mRNA level was used as reference.

the cell front during endothelial cell migration [59]. Moreover it has been shown that membrane lipids re-localize during cell polarization processes observed during cell migration and characterized by cytoskeletal reorientation and new redistribution of proteins in membranes. A well-documented example of lipid reorientation and polarization during cell migration is the lateral asymmetric distribution of phosphatidylinositol (3,4,5)-trisphosphate (PIP3) [60]. Cholesterol has also been reported to be involved in the re-localization of lipid microdomains during signaling in chemotactic cells [61]. Indeed, an asymmetric redistribution of lipid domain-associated molecules, including ganglioside GM1, to the leading edge has been reported after chemoattractant stimulations [62,63]. Those reports demonstrate accumulation of membrane cell signaling proteins in the leading edge of migrating cells [62,63] and suggest involvement of lipid microdomains as signal amplification platforms during cell polarization and migration. For instance in epithelial cells, α- and β-integrin subunits are concentrated in lipid microdomains and adhere to and communicate with extracellular matrix components (including collagen, laminins, and fibronectin) in collaboration with the actin cytoskeleton via talin, paxillin, and focal adhesion kinase (FAK) [64,65]. Similar interactions were demonstrated for example to regulate pseudopod protrusion and phagocyte migration [66]. While in several cell types lipid microdomains act through these interactions to induce morphological changes required for detachment and migration, in other cell types lipid microdomains are involved in the contraction at the trailing edge [67].

In keratinocytes, we demonstrate here that lipid microdomains' disruption decreases cell migration. However, underlying mechanisms involved in this regulation remain to be established. Interestingly, data also indicate that migration abilities decrease with senescence of keratinocytes, as is the case when SM is depleted. Further investigations are now required to elucidate how impaired lipid microdomains could be involved in reduced keratinocyte migration and thus in alterations of the re-epithelialization process observed in aged skin.

Keratinocytes organize lipid submicrometric domains while being proliferative. When becoming senescent, keratinocytes suffer from altered sphingolipid content and disappearance of SM-rich domains. One of the future challenges will be identifying if preserved SM-rich domains could prevent senescence in this cell type.

Supplementary data to this article can be found online at http://dx.doi.org/10.1016/j.bbalip.2017.06.001.

Conflicts of interest

No conflicts of interest, financial or otherwise, are declared by the authors.

Author contributions

YP, CLDR, and FDC conceived and designed the research; AM, MH, CW and VL performed experiments; AM and JR analyzed data; YP, CLDR, FDC, MH, DT, CG, KV and AM interpreted the results; AM prepared figures and drafted the manuscript; YP, CLDR, DT and FDC edited

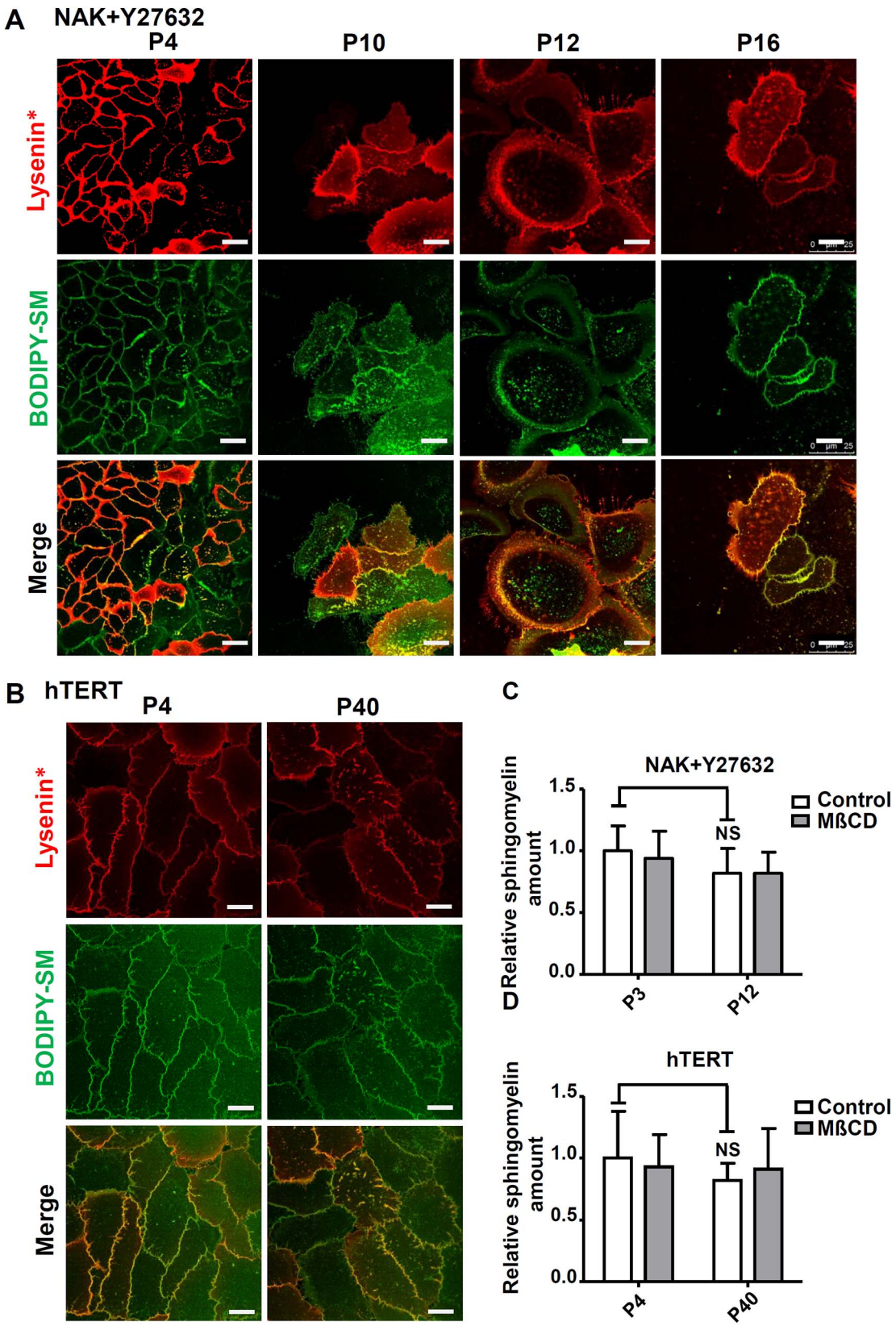

Fig. 9. SM-rich submicrometric lipid domains are preserved in Y27632-treated and in NhTERT immortalized keratinocytes: A. Human NAKs were continuously cultured in the presence or absence of 10 μM Y27632 Rho kinase inhibitor in order to prevent replicative senescence and were double-labelled by lysenin* and BODIPY-SM as previously described at increasing passages. B. NhTERT immortalized keratinocytes at low (P4) and high (P40) passages were identically double-labelled. All scale bars, 20 μm. C. and D. Sphingomyelin amount was measured in Y27632-treated NAKs and in NhTERT immortalized keratinocytes during increasing passages. Data are presented as means ± SD of three independent experiments and values have been normalized to protein concentration in each sample.

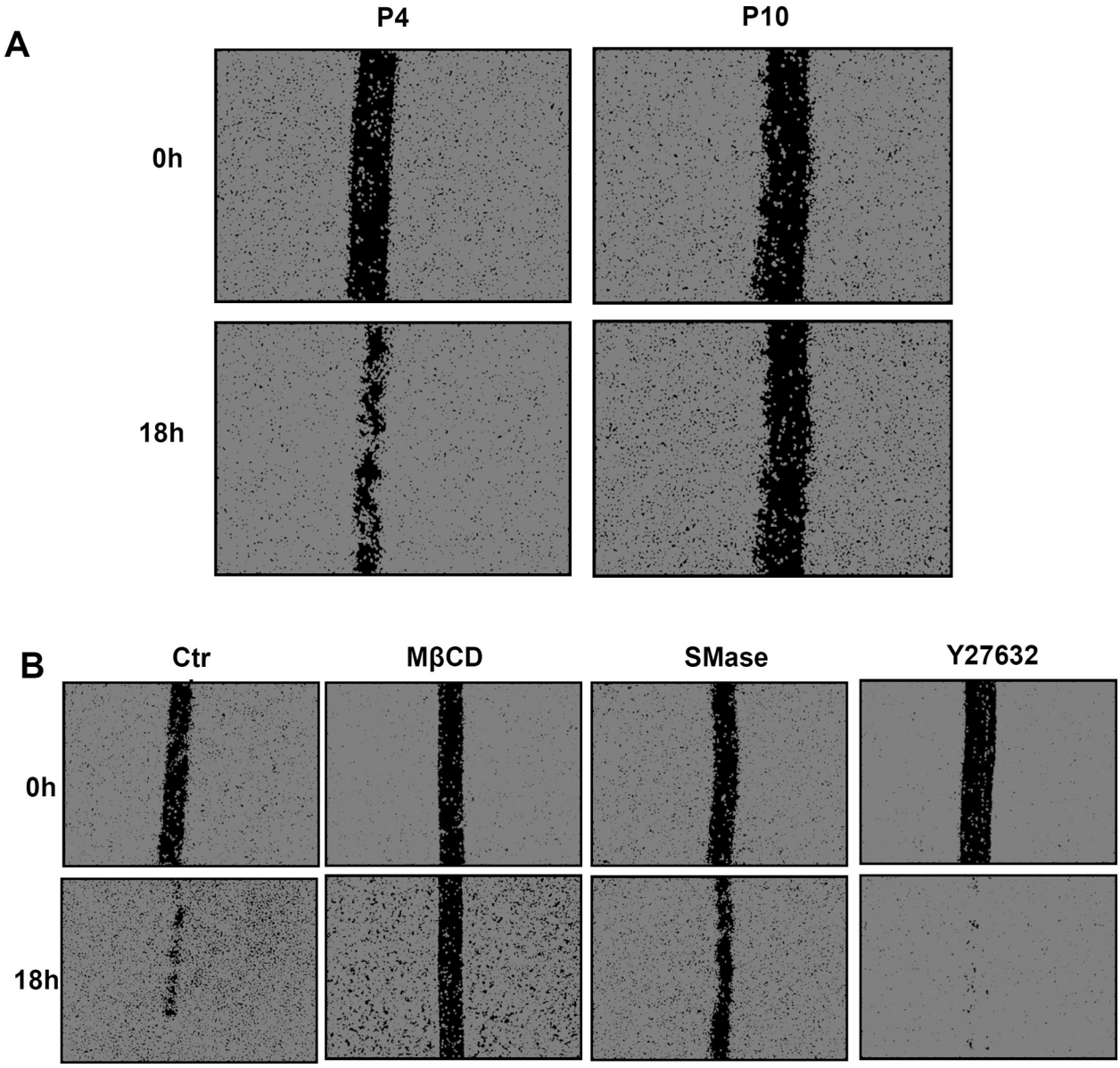

Fig. 10. The ability of keratinocytes to migrate decreases in senescent cells as well as in cells treated to deplete cholesterol or SM in membranes. A. Early passage and senescent keratinocytes were cultured to confluence, then growth-arrested by mitomycin-C before analyzing their ability to migrate by scratch wound assays. The wound closure was monitored during 18 h after cell scratch (see also Video 4). (B) Pre-senescent keratinocytes were maintained in the presence of 10 μM Y27632 Rho kinase inhibitor, or were treated with 5 mU/ml SMase or 7.5 mM MβCD to respectively deplete SM or cholesterol from their membranes, then the ability of keratinocytes to migrate in each condition was evaluated as described above (see also Video 5).

and revised final version of manuscript before approval by all authors.

Transparency document

The http://dx.doi.org/10.1016/j.bbalip.2017.06.001 associated with this article can be found, in online version.

Acknowledgments

This work was supported by the University of Namur (Namur, Belgium) and “Laboratoires Clarins” (Pontoise, France). FDC is a Research Associate of the FNRS, Belgium. The authors thank Drs. A. Miyawaki, M. Abe and T. Kobayashi at Riken Brain Science Institute (Saitama, Japan) as well as H. Mizuno (KU Leuven, Belgium) for generously supplying the Dronpa-NT-lysenin and Dronpa-theta-D4 plasmids, M. Carquin and H. Pollet (UCL, Belgium) for production and validation of mCherry-lysenin and mCherry-theta toxin fragments, as well as V. Deglas, N. Ninanne, and R. Volon for technical help. The authors also acknowledge the “Morphology-Imaging” platform of the UNamur.

References

[1] B.N. Giepmans, S.C. van Ijzendoorn, Epithelial cell-cell junctions and plasma membrane domains, Biochim. Biophys. Acta 1788 (4) (2009) 820–831.
[2] R.A. Cooper, Influence of increased membrane cholesterol on membrane fluidity and cell function in human red blood cells, J. Supramol. Struct. 8 (4) (1978) 413–430.
[3] M. Murata, et al., VIP21/caveolin is a cholesterol-binding protein, Proc. Natl. Acad. Sci. U. S. A. 92 (22) (1995) 10339–10343.
[4] R.G. Parton, A. Carozzi, J. Gustavsson, Caves and labyrinths: caveolae and transverse tubules in skeletal muscle, Protoplasma 212 (1–2) (2000) 15–23.
[5] L.J. Pike, Rafts defined: a report on the Keystone Symposium on Lipid Rafts and Cell Function, J. Lipid Res. 47 (7) (2006) 1597–1598.
[6] E. London, D.A. Brown, Insolubility of lipids in Triton X-100: physical origin and relationship to sphingolipid/cholesterol membrane domains (rafts), Biochim. Biophys. Acta 1508 (1–2) (2000) 182–195.

[7] M. Grzybek, et al., Rafts—the current picture, Folia Histochem. Cytobiol. 43 (1) (2005) 3–10.
[8] L.A. Bagatolli, To see or not to see: lateral organization of biological membranes and fluorescence microscopy, Biochim. Biophys. Acta 1758 (10) (2006) 1541–1556.
[9] M. Carquin, et al., Cholesterol segregates into submicrometric domains at the living erythrocyte membrane: evidence and regulation, Cell. Mol. Life Sci. (2015).
[10] M. Carquin, et al., Endogenous sphingomyelin segregates into submicrometric domains in the living erythrocyte membrane, J. Lipid Res. 55 (7) (2014) 1331–1342.
[11] L. D'Auria, et al., Segregation of fluorescent membrane lipids into distinct micrometric domains: evidence for phase compartmentation of natural lipids? PLoS One 6 (2) (2011) e17021.
[12] D. Tyteca, et al., Three unrelated sphingomyelin analogs spontaneously cluster into plasma membrane micrometric domains, Biochim. Biophys. Acta 1798 (5) (2010) 909–927.
[13] M. Carquin, et al., Recent progress on lipid lateral heterogeneity in plasma membranes: from rafts to submicrometric domains, Prog. Lipid Res. 62 (2016) 1–24.
[14] J. Campisi, The role of cellular senescence in skin aging, J. Investig. Dermatol. Symp. Proc. 3 (1) (1998) 1–5.
[15] M. Yaar, B.A. Gilchrest, Skin aging: postulated mechanisms and consequent changes in structure and function, Clin. Geriatr. Med. 17 (4) (2001) 617–630 (v).
[16] E. De Vuyst, et al., MbetaCD concurs with IL-4, IL-13 and IL-25 to induce alterations reminiscent of atopic dermatitis in reconstructed human epidermis, Exp. Dermatol. (2016).
[17] C. Mathay, et al., Transcriptional profiling after lipid raft disruption in keratinocytes identifies critical mediators of atopic dermatitis pathways, J. Investig. Dermatol. 131 (1) (2011) 46–58.
[18] F. Minner, F. Herphelin, Y. Poumay, Study of epidermal differentiation in human keratinocytes cultured in autocrine conditions, Methods Mol. Biol. 585 (2010) 71–82.
[19] M.A. Dickson, et al., Human keratinocytes that express hTERT and also bypass a p16(INK4a)-enforced mechanism that limits life span become immortal yet retain normal growth and differentiation characteristics, Mol. Cell. Biol. 20 (4) (2000) 1436–1447.
[20] K. Gosselin, et al., Senescent keratinocytes die by autophagic programmed cell death, Am. J. Pathol. 174 (2) (2009) 423–435.
[21] R. Jans, et al., Cholesterol depletion upregulates involucrin expression in epidermal keratinocytes through activation of p38, J. Investig. Dermatol. 123 (3) (2004) 564–573.
[22] T.D. Schmittgen, K.J. Livak, Analyzing real-time PCR data by the comparative C(T) method, Nat. Protoc. 3 (6) (2008) 1101–1108.
[23] L. D'Auria, et al., Micrometric segregation of fluorescent membrane lipids: relevance for endogenous lipids and biogenesis in erythrocytes, J. Lipid Res. 54 (4) (2013) 1066–1076.
[24] L.L. Norman, et al., Modification of cellular cholesterol content affects traction force, adhesion and cell spreading, Cell. Mol. Bioeng. 3 (2) (2010) 151–162.
[25] O.G. Ramprasad, et al., Changes in cholesterol levels in the plasma membrane modulate cell signaling and regulate cell adhesion and migration on fibronectin, Cell Motil. Cytoskeleton 64 (3) (2007) 199–216.
[26] K. Gosselin, et al., Senescence-associated oxidative DNA damage promotes the generation of neoplastic cells, Cancer Res. 69 (20) (2009) 7917–7925.
[27] G.P. Dimri, et al., A biomarker that identifies senescent human cells in culture and in aging skin in vivo, Proc. Natl. Acad. Sci. U. S. A. 92 (20) (1995) 9363–9367.
[28] F. Debacq-Chainiaux, et al., Protocols to detect senescence-associated beta-galactosidase (SA-betagal) activity, a biomarker of senescent cells in culture and in vivo, Nat. Protoc. 4 (12) (2009) 1798–1806.
[29] F. Rodier, J. Campisi, Four faces of cellular senescence, J. Cell Biol. 192 (4) (2011) 547–556.
[30] Y. Soroka, et al., Aged keratinocyte phenotyping: morphology, biochemical markers and effects of Dead Sea minerals, Exp. Gerontol. 43 (10) (2008) 947–957.
[31] E. Hara, et al., Regulation of p16CDKN2 expression and its implications for cell immortalization and senescence, Mol. Cell. Biol. 16 (3) (1996) 859–867.
[32] S. Ressler, et al., p16INK4A is a robust in vivo biomarker of cellular aging in human skin, Aging Cell 5 (5) (2006) 379–389.
[33] S. Chapman, et al., Human keratinocytes are efficiently immortalized by a Rho kinase inhibitor, J. Clin. Invest. 120 (7) (2010) 2619–2626.
[34] K. Simons, E. Ikonen, Functional rafts in cell membranes, Nature 387 (6633) (1997) 569–572.
[35] K. Simons, M.J. Gerl, Revitalizing membrane rafts: new tools and insights, Nat. Rev. Mol. Cell Biol. 11 (10) (2010) 688–699.
[36] H. Shogomori, T. Kobayashi, Lysenin: a sphingomyelin specific pore-forming toxin, Biochim. Biophys. Acta 1780 (3) (2008) 612–618.
[37] J.F. Frisz, et al., Direct chemical evidence for sphingolipid domains in the plasma membranes of fibroblasts, Proc. Natl. Acad. Sci. U. S. A. 110 (8) (2013) E613–E622.
[38] J.F. Frisz, et al., Sphingolipid domains in the plasma membranes of fibroblasts are not enriched with cholesterol, J. Biol. Chem. 288 (23) (2013) 16855–16861.
[39] H.A. Scheidt, et al., The potential of fluorescent and spin-labeled steroid analogs to mimic natural cholesterol, J. Biol. Chem. 278 (46) (2003) 45563–45569.
[40] M. Maekawa, G.D. Fairn, Complementary probes reveal that phosphatidylserine is required for the proper transbilayer distribution of cholesterol, J. Cell Sci. 128 (7) (2015) 1422–1433.
[41] K. Roepstorff, et al., Sequestration of epidermal growth factor receptors in non-caveolar lipid rafts inhibits ligand binding, J. Biol. Chem. 277 (21) (2002) 18954–18960.
[42] T. Ringerike, et al., Cholesterol is important in control of EGF receptor kinase activity but EGF receptors are not concentrated in caveolae, J. Cell Sci. 115 (Pt 6) (2002) 1331–1340.
[43] P. Drochmans, et al., Structure and biochemical composition of desmosomes and tonofilaments isolated from calf muzzle epidermis, J. Cell Biol. 79 (2 Pt 1) (1978) 427–443.
[44] S.N. Stahley, et al., Desmosome assembly and disassembly are membrane raft-dependent, PLoS One 9 (1) (2014) e87809.
[45] M.P. Mattson, R.G. Cutler, Sphingomyelin and ceramide in brain aging, neuronal plasticity and neurodegenerative disorders, Advances in Cell Aging and Gerontology, Elsevier, 2003, pp. 97–115.
[46] R.G. Cutler, et al., Involvement of oxidative stress-induced abnormalities in ceramide and cholesterol metabolism in brain aging and Alzheimer's disease, Proc. Natl. Acad. Sci. U. S. A. 101 (7) (2004) 2070–2075.
[47] J. Rogers, et al., Stratum corneum lipids: the effect of ageing and the seasons, Arch. Dermatol. Res. 288 (12) (1996) 765–770.
[48] A.B. Cua, K.P. Wilhelm, H.I. Maibach, Skin surface lipid and skin friction: relation to age, sex and anatomical region, Skin Pharmacol. 8 (5) (1995) 246–251.
[49] V. Schreiner, et al., Barrier characteristics of different human skin types investigated with X-ray diffraction, lipid analysis, and electron microscopy imaging, J. Investig. Dermatol. 114 (4) (2000) 654–660.
[50] R.E. Mouton, M.E. Venable, Ceramide induces expression of the senescence histochemical marker, beta-galactosidase, in human fibroblasts, Mech. Ageing Dev. 113 (3) (2000) 169–181.
[51] M.E. Venable, et al., Role of ceramide in cellular senescence, J. Biol. Chem. 270 (51) (1995) 30701–30708.
[52] V.J. Cristofalo, et al., Alterations in the responsiveness of senescent cells to growth factors, J. Gerontol. 44 (6) (1989) 55–62.
[53] T. Matsuda, et al., Decreased response to epidermal growth factor during cellular senescence in cultured human microvascular endothelial cells, J. Cell. Physiol. 150 (3) (1992) 510–516.
[54] H. Shiraha, et al., Aging fibroblasts present reduced epidermal growth factor (EGF) responsiveness due to preferential loss of EGF receptors, J. Biol. Chem. 275 (25) (2000) 19343–19351.
[55] J. Campisi, Aging, cellular senescence, and cancer, Annu. Rev. Physiol. 75 (2013) 685–705.
[56] M. Yaar, B.A. Gilchrest, Ageing and photoageing of keratinocytes and melanocytes, Clin. Exp. Dermatol. 26 (7) (2001) 583–591.
[57] L.M. Pierini, et al., Membrane lipid organization is critical for human neutrophil polarization, J. Biol. Chem. 278 (12) (2003) 10831–10841.
[58] P.K. Ghosh, et al., Membrane microviscosity regulates endothelial cell motility, Nat. Cell Biol. 4 (11) (2002) 894–900.
[59] A. Vasanji, et al., Polarization of plasma membrane microviscosity during endothelial cell migration, Dev. Cell 6 (1) (2004) 29–41.
[60] L. Stephens, L. Milne, P. Hawkins, Moving towards a better understanding of chemotaxis, Curr. Biol. 18 (11) (2008) R485–R494.
[61] C. Gomez-Mouton, et al., Dynamic redistribution of raft domains as an organizing platform for signaling during cell chemotaxis, J. Cell Biol. 164 (5) (2004) 759–768.
[62] S. Mañes, et al., Membrane raft microdomains mediate front-rear polarity in migrating cells, EMBO J. 18 (22) (1999) 6211–6220.
[63] C. Gomez-Mouton, et al., Segregation of leading-edge and uropod components into specific lipid rafts during T cell polarization, Proc. Natl. Acad. Sci. U. S. A. 98 (17) (2001) 9642–9647.
[64] A.L. Berrier, K.M. Yamada, Cell–matrix adhesion, J. Cell. Physiol. 213 (3) (2007) 565–573.
[65] J.G. Lock, B. Wehrle-Haller, S. Strömblad, Cell–matrix adhesion complexes: master control machinery of cell migration, Semin. Cancer Biol. 18 (1) (2008) 65–76.
[66] R. Corriden, P.A. Insel, New insights regarding the regulation of chemotaxis by nucleotides, adenosine, and their receptors, Purinergic Signal. 8 (3) (2012) 587–598.
[67] J.S. Mitchell, et al., Clustering T-cell GM1 lipid rafts increases cellular resistance to shear on fibronectin through changes in integrin affinity and cytoskeletal dynamics, Immunol. Cell Biol. 87 (4) (2009) 324–336.